Proc. Natl. Acad. Sci. USA
Vol. 94, pp. 4250–4255, April 1997
Chemistry

The crystal structure of subtilisin Carlsberg in anhydrous dioxane and its comparison with those in water and acetonitrile

JENNIFER L. SCHMITKE, LAWRENCE J. STERN, AND ALEXANDER M. KLIBANOV*

Department of Chemistry, Massachusetts Institute of Technology, Cambridge, MA 02139

Contributed by Alexander M. Klibanov, March 3, 1997

ABSTRACT **The x-ray crystal structure of the serine protease subtilisin Carlsberg in anhydrous dioxane has been determined to 2.6-Å resolution. The enzyme structure is found to be nearly indistinguishable from the structures previously determined in water and acetonitrile. Small changes in the side-chain conformations between the dioxane and water structures are of the same magnitude as those observed between two structures in different aqueous systems. Seven enzyme-bound dioxane molecules have been detected, each potentially forming at least one hydrogen bond with a subtilisin hydrogen-bond donor or bound water. Two of the bound dioxane molecules are in the active-site region, one in the P2 and another bridging the P1′ and P3′ pockets. The other five dioxane molecules are located on the surface of subtilisin at interprotein crystal contacts. The locations of the bound solvent in the dioxane structure are distinct from those in the structures in acetonitrile and in water.**

Enzymatic catalysis in organic medium has emerged as an important area of research in biotechnology and bioorganic chemistry (1). The structure of enzymes in such milieu should aid in the understanding and optimization of this catalysis. Several years ago, we succeeded in determining the first such x-ray crystal structure, that of subtilisin Carlsberg in anhydrous acetonitrile (2). It was found that the structure of the lightly cross-linked enzyme crystal in the anhydrous solvent was virtually indistinguishable from that in water (2, 3). This conclusion was corroborated by subsequent crystallographic studies of two other enzymes—γ-chymotrypsin in hexane (4, 5) and elastase in acetonitrile (6).

To date (2–6) only one nonaqueous solvent has been examined for each crystalline enzyme. A rationale has been tentatively adopted (7–9) that if the enzyme structure does not change upon transition from water to acetonitrile or hexane, then it also should not change upon transition to another solvent because the difference in physicochemical properties between two organic solvents should be less than between water and an organic solvent. However, a direct validation of this reasoning until now has been missing.

In the present study, we have determined the x-ray crystal structure of lightly cross-linked subtilisin in a second unrelated anhydrous solvent, dioxane. This structure has turned out to be essentially the same as those in water (3) and in acetonitrile (2). Interestingly, the locations of the subtilisin-bound dioxane and acetonitrile molecules are distinct.

MATERIALS AND METHODS

Crystal Preparation. Subtilisin Carlsberg (serine protease from *Bacillus licheniformis*, EC 3.4.21.14) was purchased from Sigma. Crystals were grown from an aqueous 330 mM cacodylate buffer (pH 5.6) saturated with Na_2SO_4, approximately 13% (10). A single crystal (~0.8 × 0.1 × 0.05 mm) was placed in 1 ml of a 10% glutaraldehyde cross-linking solution containing 30 mM cacodylate buffer (pH 7.5) and 10% Na_2SO_4. The glutaraldehyde solution was aged for 3 days at room temperature before reaction. (Crystal appearance and diffraction limit were dependent on the glutaraldehyde aging protocol.) We presume a relatively low extent of cross-linking: there are only nine lysine residues in subtilisin and only five that could reasonably be involved in an intermolecular cross-linking event (distances less than 20 Å). No glutaraldehyde or modified Lys electron density was detected in the electron density maps.

The crystal was incubated in the cross-linking solution for 30 min and washed five times with 2 ml of distilled water. The water was then removed from the crystal and replaced with anhydrous dioxane by washing five times (each with 2 ml of anhydrous dioxane). The crystal was left in the solvent for 20 min after each wash. Finally, the crystal was mounted in a 0.5-mm-diameter quartz capillary for data collection. The water content of similarly treated crystals was found to be 3% (wt/wt) with a Mettler Karl–Fischer titrimeter (11).

Data Collection and Reduction. X-ray diffraction data were obtained at ambient temperature (23 ± 2°C) to a nominal resolution of 2.6 Å with an RAXIS II area detector. X-rays were generated with a Rigaku RU200 rotating copper anode source, and the Cu K_α radiation was selected with a graphite monochromator. An oscillation range of 1.75° with an exposure time of 35 min was used to collect data over a total of 137° (>95% of the possible data 14–2.6 Å). The reflections were indexed and the intensities were integrated and scaled with DENZO and SCALEPACK of the HKL Package (Z. Otinowski and W. Minor, personal communication). Data collection statistics are presented in Table 1. Structure factor magnitudes were calculated from the intensities and truncated with programs in the CCP4 Suite (12).

Space Group Determination. Pseudoprecession pictures were generated revealing two-fold rotation axes on *h*, *k*, and *l*, placing the crystal in the 222 rotation group. Systematic extinctions revealed *h* to be a screw axis, whereas *k* and *l* remained ambiguous. Thus, the possible space groups at this point were $P222_1$, $P2_12_12$, and $P2_12_12_1$. Molecular replacement translation searches (see below) only yielded a real solution, a peak of 12.8σ, in the $P2_12_12_1$ space group; no peaks were found above 7.0σ for the other space groups. Thus, the space group was $P2_12_12_1$, the same space group as that of the cross-linked crystal in both water and acetonitrile.

Molecular Replacement. Initial phases were determined by molecular replacement using the program AMORE (13) in the

The publication costs of this article were defrayed in part by page charge payment. This article must therefore be hereby marked "*advertisement*" in accordance with 18 U.S.C. §1734 solely to indicate this fact.

0027-8424/97/944250-6$2.00/0
PNAS is available online at **http://www.pnas.org**.

Data deposition: The atomic coordinates and structure factors have been deposited in the Protein Data Bank, Chemistry Department, Brookhaven National Laboratory, Upton, NY 11973 [reference 1af4 (coordinates) and r1af4sf (structure factors)]. Dioxane parameter and topology files are available from the *X-PLOR Topology and Parameter Library for Hetero Compounds* at http://xplor.csb.yale.edu/hetero.

*To whom reprint requests should be addressed. e-mail: klibanov@mit.edu.

Table 1. Crystal properties, data collection, refinement, and model statistics

Crystal properties		
Space group	$P2_12_12_1$	
Cell dimensions, ($a \times b \times c$), Å	77.0 × 55.2 × 53.9	
Molecules per asymmetric unit, no.	1	
Data collection statistics	Resolution limits	
	14–2.6 Å	2.7–2.6 Å
Measurements, no.	39,403	3,891
Unique reflections, no.	7,111	745
Completeness, %	95.9	96.2
Mean I/σ_I	6.2	4.3
R_{merge}, %	14.2	38.7
Crystallographic refinement statistics	Resolution limits	
	6.0–2.6 Å	2.7–2.6 Å
Reflections, no.	6,554	745
Reflections with $F > 2\sigma_F$, no.	6,307	708
Crystallographic R factor, %	16.1	19.3
Free R factor, %	24.6	28.0
Model statistics		
Total no. of nonhydrogen atoms	2017	
Protein atoms, no.	1910	
Solvent atoms, no.	107	
RMSD bond length, Å	0.014	
RMSD bond angle, degrees	1.66	
Mean B factor (SD), Å^2		
Protein	12.5 (5.9)	
Solvent	22.8 (12.3)	
Mean real space fit (SD), %		
Protein	89.7 (3.8)	
Solvent	83.1 (6.6)	

Unit cell dimensions for the cross-linked crystal are 77.2 × 55.8 × 53.7 Å in water (3) and 77.1 × 55.4 × 53.6 Å in acetonitrile (2) and for the non-cross-linked crystal in aqueous buffer are 76.7 × 55.6 × 53.1 Å (10). R_{merge} is the R factor on the intensity for symmetry-related measurements. The crystallographic R factor is the R factor on structure factors for reflections used in the refinement (90% of total). The free R factor is the R factor on structure factors for reflections randomly omitted from the refinement and used as the test set (10% of total). In model statistics, only atoms included in the refinement are shown. A Luzzati analysis revealed the average coordinate error to be 0.3 Å. RMSD is rms deviation from ideal geometric values [Enge and Huber parameter set (27)]. The mean real space fit is the real-space-fit values calculated from the $2F_o$–F_c electron density maps.

CCP4 Suite with the 2.75-Å subtilisin structure in aqueous buffer reported by Neidhart and Petsko (10) as the search model. The rotation search using the 10- to 4.0-Å data revealed one unique solution at 9.7σ (standard deviation above the mean rotation function). The translation search in the $P2_12_12_1$ space group yielded a single peak of 12.8σ. Comparison of the molecular replacement solution to that of the original search model showed that the root mean square (rms) displacement was only 0.001 Å, i.e., no significant crystal rearrangement was observed for the cross-linking and solvent transfer steps. A series of $2F_o$–F_c maps were calculated by using phases determined from models that had sequential regions omitted (11% of the total atoms). The omit maps showed clear density for all omitted regions with the exception of residues 158–162 (see below).

Refinement and Model Building. After molecular replacement, the R factor for the search model was 0.30 for all the reflections in the 6.0- to 2.6-Å resolution shell and the R free (14), consisting of reflections that are left out of the refinement (10% of total), was 0.32. The search model was first rebuilt residue by residue into the omitted regions by using the omit maps generated as above, adjusting side-chain torsion angles and occasionally changing residue rotamers. Approximately 25% of the residues required some adjustment to center them in their electron density. Two rounds of refinement using X-PLOR (15) followed by manual rebuilding using the program O (16) were then performed on the protein structure. The refinement protocol in X-PLOR consisted of a rigid-body refinement (40 cycles using the 10- to 4.0-Å data) followed by simulated annealing (6.0–2.6 Å), a conventional positional refinement (50 cycles, 6.0–2.6 Å), and a restrained group B factor refinement (20 cycles, 6.0–2.6 Å). The simulated annealing runs involved heating to 3,000 K and then cooling in increments of 25 K with 50 steps of molecular dynamics simulations for 0.5 fs at each temperature. At this stage, the R factor and R free were brought down to 0.22 and 0.30, respectively, in the 6.0- to 2.6-Å resolution shell.

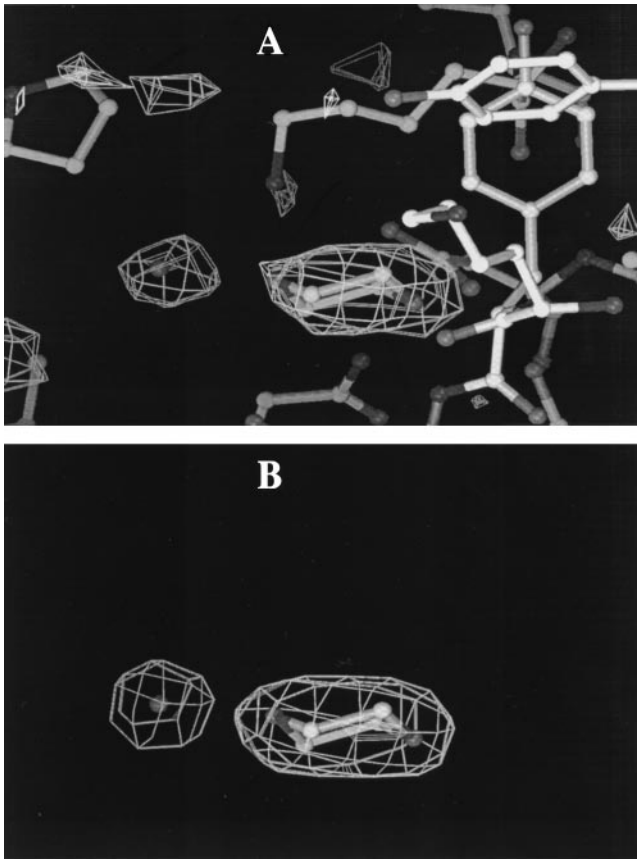

FIG. 1. (*A*) Ball-and-stick model of a dioxane molecule and a water molecule binding at a subtilisin crystal contact. Carbon, oxygen, and nitrogen are depicted in white, light gray, and dark gray, respectively. $|F_o$–$F_c|\phi_{calc}$ map, omitting solvent molecules, is shown in white at the 3σ contour. (*B*) The solvent molecules are displayed as in *A*; shown in white is the F_c theoretical electron density map for the water and dioxane molecules.

Subtilisin contains a flexible surface loop, Asn-158 to Thr-162, for which initially very weak density was observed. This entire loop was omitted during the early refinement cycles. Residues of the loop were gradually included in the model in later refinement rounds. However, Ser-159 and Gly-160 did not have well-defined electron density even in the final maps, and they were, therefore, not included in the final model. This loop also appears to be very flexible in the cross-linked crystal in water, reflected by high B factors of residues 158–162.

Solvent Molecules. Two rounds of manual building in O (16) and refinement with X-PLOR (15) were performed resulting in the addition of the first 35 waters. Potential waters were located with the F_o–F_c electron density map at the 3.0σ contour level (17). Initially, they were only built into density peaks that clearly exhibited the appropriate shape; any peaks that were

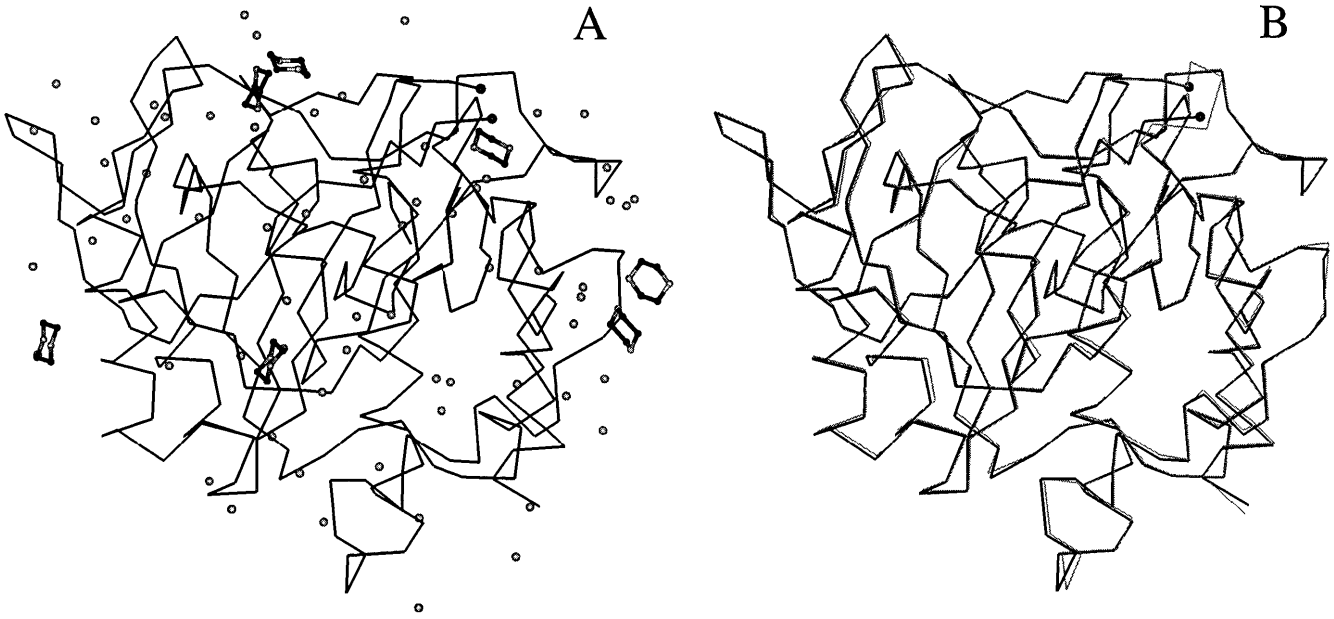

FIG. 2. (*A*) C_α trace of the protein structure of subtilisin Carlsberg in anhydrous dioxane (black lines) with bound water (gray balls) and dioxane (balls-and-sticks: C atoms in black and O atoms in gray) molecules. (*B*) Superimposition of the C_α traces of subtilisin in water (thin gray lines) and in anhydrous dioxane (thicker black lines). The rms shifts of the C_α atoms and of the main-chain atoms are 0.31 Å and 0.33 Å, respectively. Ser-159 and Gly-160 are not included in the model of subtilisin in dioxane because of uncertainties in their location; the C_α atoms of Asn-158 and Ser-161 are shown as balls (upper right).

possibly due to dioxane molecules were excluded. The refinement protocol using X-PLOR was the same as described above. Potential waters were retained if their electron density in subsequent $2F_o$–F_c maps (17) persisted after the simulated annealing refinement and if they fulfilled the following criteria: within 3.4 Å of a subtilisin oxygen or nitrogen atom (or bound water in the second round) with good hydrogen-bonding geometry, *B* factors less than 45 Å^2, and real-space-fit correlation coefficients above 65%. After inclusion of these 35 waters, the *R* factor and *R* free were brought down to 0.286 and 0.167, respectively, for the data in the 6.0- to 2.6-Å resolution shell. Three rounds of manual building in O and refinement with the program REFMAC were carried out resulting in the inclusion of 30 additional waters, for a total of 65 water molecules in the model. The water identification and manual building was performed as above, but the refinement was done with REFMAC, where a combined positional and a restrained individual *B* factor refinement was performed with the maximum likelihood residual and all the working data, 14–2.6 Å. Criteria for acceptable waters were the same as above. The inclusion of the final 30 waters resulted in an improvement in *R* free to 0.276 with no change in the *R* factor (0.167).

Dioxane molecules were introduced into the model by means of four rounds of manual building in O and automatic refinement using X-PLOR. The dioxane model used has a chair conformation as reported by Buschmann *et al.* (18) for the phase I crystal at 279 K. The dioxane parameter and topology files for X-PLOR were generated with XPLO2D.† Potential dioxane molecules were located by using the F_o–F_c map. Electron density was considered to represent a potential dioxane if the peak was above 3.0σ with at least one dioxane oxygen within hydrogen-bonding distance to a hydrogen-bond donor on the protein or water (Fig. 1*A*). Dioxane electron density was recognized by comparison with F_c maps calculated for a theoretical dioxane molecule between the resolution limits of 14–2.6 Å (Fig. 1*B*). A complication that must be noted is that the electron density for a single dioxane molecule at this resolution appears similar to the density for two hydrogen-bonded water molecules (the O–O distance in dioxane is 2.68 Å). In a few cases, the hydrogen-bonding pattern in the model was consistent only with two waters; however, when it was ambiguous, the following criteria were used to distinguish between the possibilities of the density corresponding to one dioxane or two waters. Initially, a real-space-fit correlation coefficient was calculated for both a dioxane molecule and two waters built into such an electron density peak. A conventional positional refinement for 40 cycles, followed by a restrained individual *B* factor refinement for 20 cycles (both using the 6.0- to 2.6-Å data) was performed with X-PLOR (15) on the model with either one dioxane molecule or two waters. The respective real-space-fit and *R* free values were calculated; dioxane molecules were kept only if these parameters, before and after refinement, were superior to those for the two waters. Furthermore, putative dioxane molecules with average *B* factors greater than 50 Å^2 or real-space-fit correlation coefficients less than 60% were discarded. Seven dioxane molecules were included in the final model. The final *R* factor and *R* free for the 6.0- to 2.6-Å resolution shell were 0.161 and 0.246, respectively (Table 1).

Structure Comparisons. The structure of subtilisin Carlsberg in dioxane was superimposed with the previously determined structures in distilled water (3) and acetonitrile (2) using LSQMAN‡ to minimize the rms distance of the main-chain atoms between the appropriate pair of structures. The rms distances between subtilisin in dioxane and in distilled water and between dioxane and acetonitrile were 0.33 and 0.36 Å, respectively. The identification of the binding pockets in the enzyme active site was accomplished by superimposition (as above) with the structure of subtilisin bound to the protease inhibitor eglin c (19). Surface area calculations were performed with the Connolly algorithm (20) with a probe radius of 1.4 Å in the INSIGHT II package from Biosym. The percentages of the exposed surface areas of the dioxane and acetonitrile molecules in their respective structures were calculated as follows: the surface area (Å^2) of a given bound dioxane or acetonitrile molecule in the structure was calculated and then

†Kleywegt, G. J. (1995) *ESF/CCP4 Newsletter*, No. 32.

‡Kleywegt, G. J. (1994) *ESF/CCP4 Newsletter,* No. 31.

expressed as a percentage of the surface area (Å^2) calculated for the free dioxane or acetonitrile molecule. The crystal contacts, as well as the rms deviations from ideality of the model, were determined by using the geometric analysis features in X-PLOR (15).

The number of intramolecular hydrogen bonds in subtilisin was determined with the program HBPLUS (I. McDonald, D. Naylor, D. Jones, and J. M. Thornton, personal communication). Hydrogen bonds were considered to exist between hydrogen-bond donor and acceptor atoms if the distance between them was less than 3.4 Å and the donor–hydrogen-acceptor angle was greater than 90°.

RESULTS AND DISCUSSION

The structure of subtilisin Carlsberg in anhydrous dioxane determined to 2.6-Å resolution (Table 1) includes 65 bound water molecules and 7 bound dioxane molecules (Fig. 2*A*). The protein structure is virtually identical to that in water (3) (Fig. 2*B*), with rms shifts for the main-chain atoms of 0.33 Å. Not only does the overall global structure of the enzyme not change upon transition from water to anhydrous dioxane, but the local side-chain structure is also essentially unaffected. Small deviations in the side-chain conformations in dioxane compared with the conformations in water are no greater than those between two previously determined structures in water, namely, those of subtilisin in the cross-linked crystal in distilled water (3) and in the non-cross-linked crystal in aqueous buffer (10). In addition, the apparent number of the intramolecular hydrogen bonds of subtilisin in dioxane and in water were found to be similar—45 and 49, respectively. Fig. 3*A* illustrates that both the overall *B* factor and the *B* factor trends through the protein are also similar in water, dioxane, and acetonitrile.

Studies involving molecular dynamics simulations have suggested that proteins in organic solvents should possess a diminished overall exposed surface area relative to their structures in water (21, 22). We observed (Fig. 3*B*) no significant change in the overall surface area of subtilisin in dioxane (9,100 Å^2) compared with water (9,100 Å^2). Additionally, there is only some 1% difference in the surface area in acetonitrile (9,000 Å^2) compared with water (Fig. 3*C*). The simulation studies (21, 22) also predict that nonpolar residues will be more exposed and polar residues less exposed in organic solvents compared with water. Although some subtilisin residues agree with this prediction, others do not. In general, the differences appear random: the average change in the exposed surface area for a given residue type does not follow the predicted trend for the structures in either dioxane or acetonitrile compared with water (Fig. 3 *B* and *C*). These inconsistencies could have arisen because the simulation studies (21, 22) were performed on a different protein, bovine pancreatic trypsin inhibitor, and in a different non-hydrogen-bonding solvent, chloroform. An alternative possibility is that the enzyme is kinetically trapped in the same conformation as in water and consequently cannot reach a minimum energy state of the sort predicted by the molecular dynamics simulations.

Since subtilisin exhibits markedly different catalytic activity and other properties in different solvents (7–9, 23), its active-site structure in solvents is a critical issue in our study. We find that, in addition to the global enzyme structure, this region in particular in the lightly cross-linked crystals of subtilisin in dioxane is essentially the same as in water. The rms displacement is 0.17 Å for all the atoms within a 10-Å radius of the head nucleophile Ser-221. Hence, the organic solvent does not alter subtilisin's catalytic activity by causing a significant structural change in the active site.

Examination of the solvent bound in the active-site region in dioxane compared with that in water (Fig. 4*A*) reveals that the catalytic water molecule, a hallmark of the active site of subtilisin and other serine proteases (24), is also present in

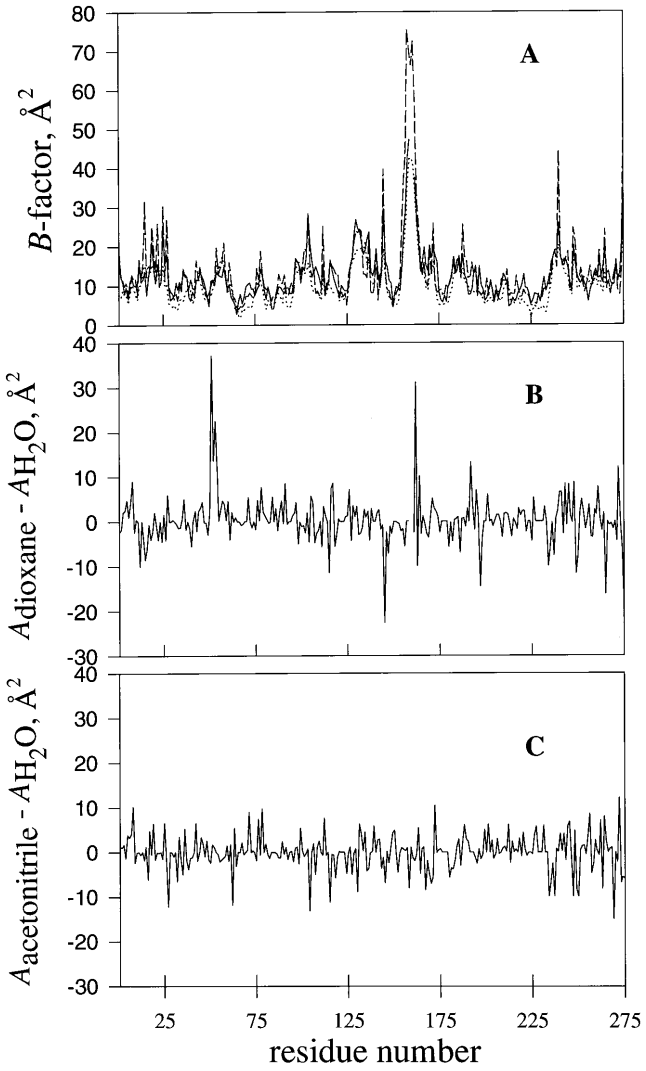

FIG. 3. (*A*) Refined crystallographic *B* factors (residue average) of subtilisin Carlsberg in dioxane (solid line), water (dashed line), and acetonitrile (dotted line). The difference in the exposed surface areas of subtilisin between dioxane and water (*B*) and between acetonitrile and water (*C*). As in Fig. 2, Ser-159 and Gly-160 are left out in *A* and *B*.

dioxane. One can speculate that in a transesterification or another nonhydrolysis reaction catalyzed by proteases in organic solvents (1), this bound water may, in fact, lead to a hydrolysis product in the first turnover. Inspection of Fig. 4*A* also shows that one dioxane molecule replaces two water molecules and one dioxane is located in an unoccupied site relative to the water structure. Additionally, some water molecules are observed in different locations in the two structures. An analogous study carried out for the situation in dioxane compared with acetonitrile (Fig. 4*B*) reveals that in the former a dioxane molecule binds in an analogous position to a bound acetonitrile, the other dioxane replaces a water molecule, and two waters replace two bound acetonitriles. The distinct solvation of the subtilisin active site in different organic solvents possibly contributes to the altered enzymatic activity and other properties in those media (7–9, 23).

Crystals of subtilisin, even after cross-linking, usually fail to diffract x-rays upon replacement of their interstitial water by most anhydrous solvents (ref. 3; unpublished results). The crystal lattice is held together by weak intermolecular interactions between the packed proteins (25). Presumably, most solvents disrupt these interactions, thereby causing the crystal to lose its integrity. We have ruled out the possibility of

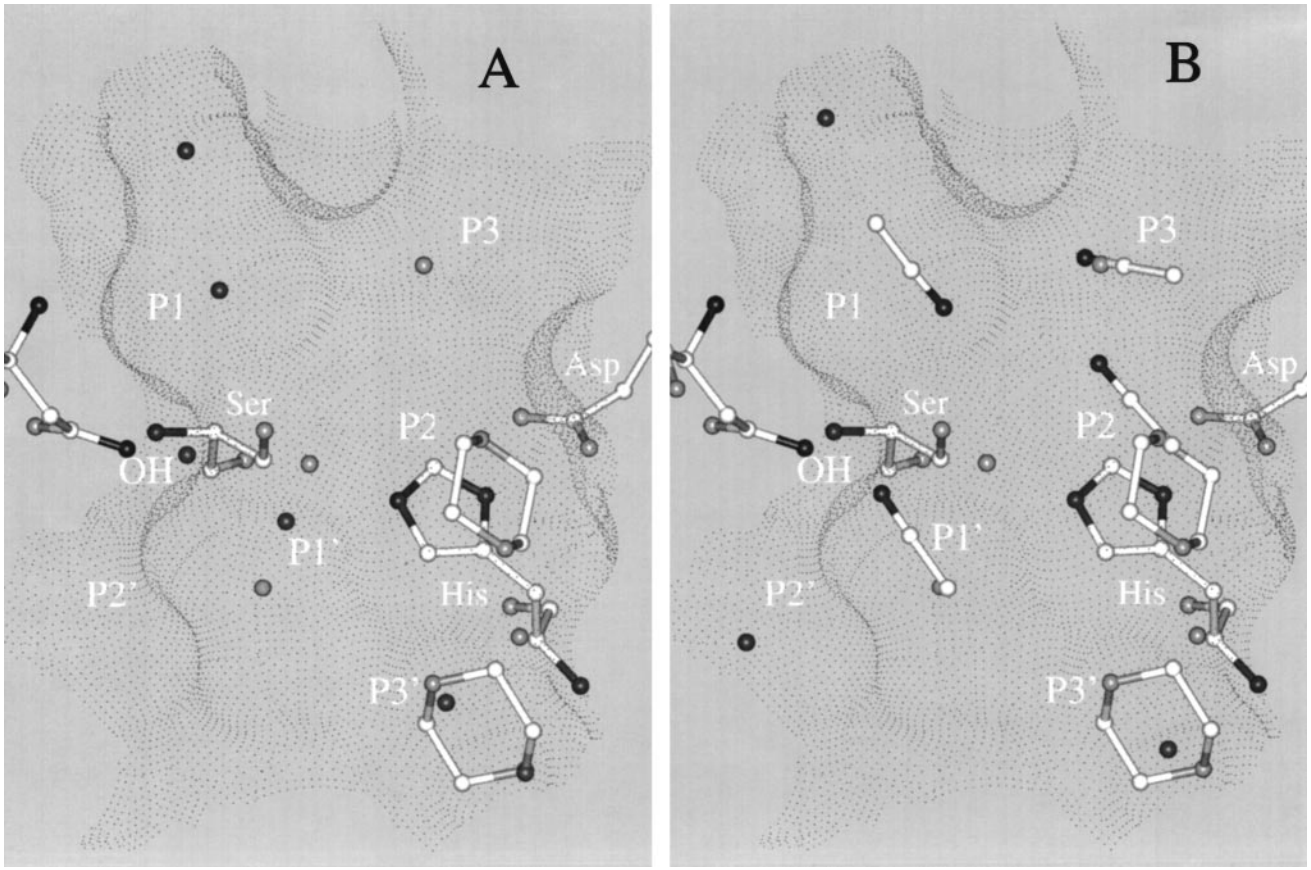

FIG. 4. Active site of subtilisin Carlsberg in anhydrous dioxane compared with that in water (*A*) and acetonitrile (*B*). The catalytic triad, Asn-155 of the oxyanion hole (OH), and solvent molecules in the dioxane structure are shown as balls-and-sticks with carbon, oxygen, and nitrogen shown in white, light-gray, and black, respectively. The water molecules in the aqueous and acetonitrile structures are depicted as dark-gray balls in *A* and *B*. The acetonitrile molecules in that structure (*B*) are also shown as linear balls-and-sticks. The surface of the protein [Connolly algorithm (20)] in the active-site region in the dioxane structure is portrayed by black dots.

significant *intramolecular* distortions: not only are the crystals catalytically active in solvents in which they fail to diffract (9), but, in fact, the activities of non-cross-linked and cross-linked crystals of subtilisin in acetonitrile are the same (2). It is, therefore, important to assess the effect of dioxane on the crystal contact regions. We observed no significant difference in the direct protein–protein crystal contacts between the dioxane and aqueous structures or between the dioxane and acetonitrile structures. It is of possible significance that of seven bound dioxanes, five are involved in crystal contacts and the other two are in the active site. Of the five, two dioxanes replace two waters, another two replace one water, and one is in a location unoccupied in the structure in water. Perhaps the subtilisin crystal remains intact in dioxane because the molecules of the latter sustain interactions (Fig. 5) maintained by the water that they replace. Likewise, the enzyme crystal should not diffract in solvents that do not preserve these interactions, e.g., toluene and octane (unpublished results), as well as several others (3).

There is an interest in determining the potential binding sites in proteins for small organic molecules representing particular functional groups, with the eventual goal of designing tightly binding compounds consisting of a combination of such groups (2, 6, 26). We therefore examined subtilisin's binding sites for dioxane and for acetonitrile and compared them. When a solvent molecule binds to the protein surface, only a fraction of the former would be in direct contact with the protein, thus leaving a significant percentage of the molecule exposed. The average exposed surface areas of the seven dioxane and 12 acetonitrile molecules are 34% and 51%, respectively. The value for the dioxane molecules must be lower because of their involvement in the crystal contacts where the dioxane molecules tend to be sandwiched between two neighboring subtilisins (Fig. 5). Thus it appears that both dioxane and acetonitrile bind at the surface of the enzyme. Meanwhile, only one dioxane molecule binds near an acetonitrile site in the respective structures (Fig. 4*B*). One dioxane molecule replaces two waters, and two dioxane molecules replace one water each (an example is in Fig. 4*B*). In contrast, three acetonitrile molecules replace one water molecule each [two in the active site (Fig. 4*B*)]. Since the dioxane and acetonitrile molecules replace *different* water molecules in their respective structures, it follows that the two solvents bind to distinct sites on subtilisin.

The question arises about the driving force of the binding of dioxane to subtilisin. A likely major contributor is hydrogen bonding—all the bound dioxanes can form at least one hydrogen bond with a subtilisin hydrogen-bond donor or an enzyme-bound water. Moreover, all but one of the bound dioxanes can form at least two hydrogen bonds, where each of the dioxane oxygen atoms is involved in at least one hydrogen bond (Fig. 5). A principal force in the acetonitrile binding to the protein surface also may be hydrogen bonding: all but 1 of the 12 bound acetonitrile molecules can form hydrogen bonds with donor atoms of subtilisin or water (allowing for the ambiguity in acetonitrile orientation in electron density maps) (2).

Since the enzyme-bound dioxane molecules that are not in the active-site region of subtilisin are found at crystal contacts, they can form more contacts with the protein than they could have in other areas of subtilisin's surface. Consequently, these dioxane molecules might be more ordered and, therefore, have more pronounced electron density. Interestingly, four of the

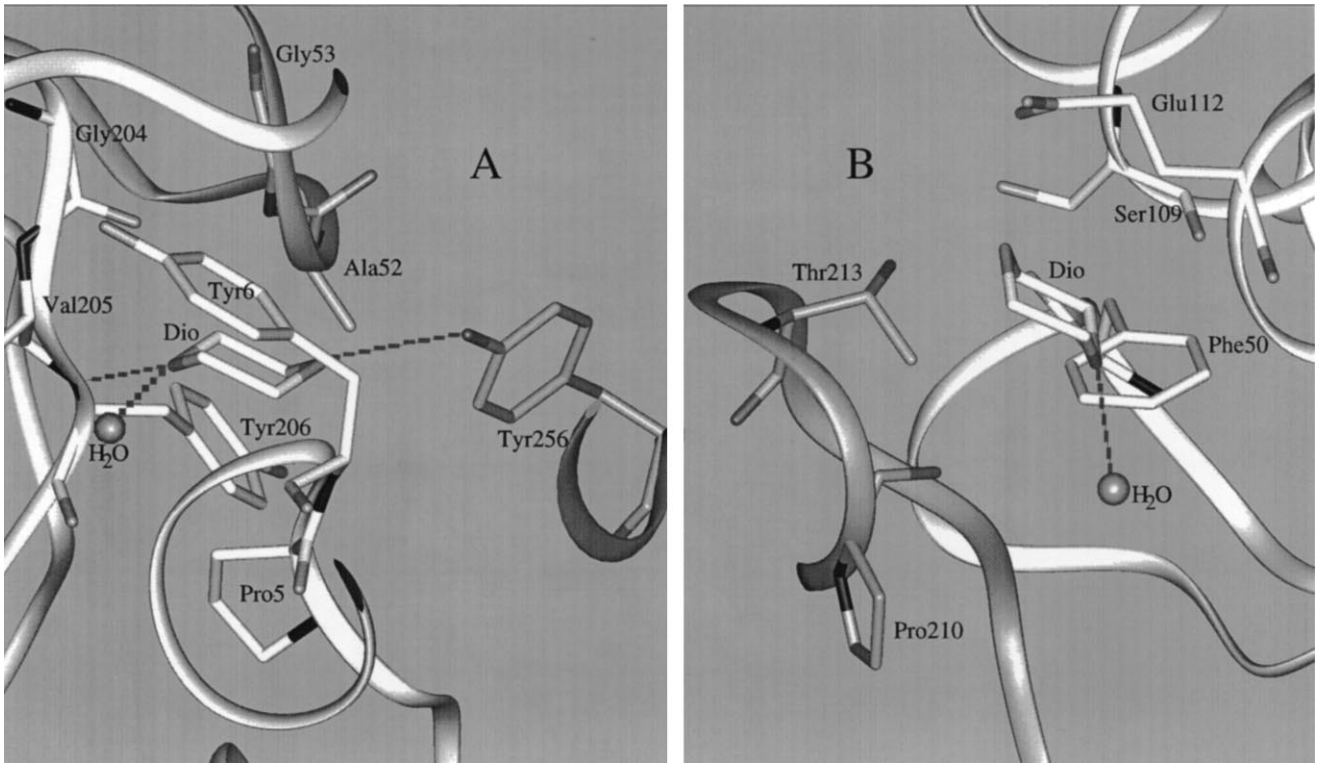

FIG. 5. Two examples of dioxane (Dio) molecules binding to subtilisin Carlsberg in anhydrous dioxane. (*A*) A dioxane molecule is seen interacting with Pro-5, Tyr-6, Gly-204, Val-205, Tyr-206, and a water molecule and with Ala-52 and Gly-53 of one neighboring symmetry-related subtilisin molecule, as well as Tyr-256 of another. (All residues depicted are within 3.5 Å of the dioxane.) (*B*) A dioxane molecule is displayed interacting with Phe-50, Ser-109, Glu-112, and a water molecule and with Pro-210 and Thr-213 of a neighboring subtilisin molecule. In both *A* and *B*, the central subtilisin's residues and bound solvent molecules mentioned above are displayed as balls-and-sticks where the carbon, oxygen, and nitrogen are white, light-gray, and black, respectively; the ribbon diagram of the subtilisin backbone is also white. The neighboring symmetry-related subtilisin's residues and ribbons are shown in darker gray colors. The hydrogen bonds, in which the dioxane oxygen atoms could be involved, are shown as gray dashed lines.

seven enzyme-bound dioxane molecules interact with a Tyr residue (Fig. 5*A*), although Tyr residues constitute less than 8% of subtilisin's amino acid residues with an exposed surface area above 30%. (On the other hand, only 5 of the 65 bound water molecules in the dioxane structure interact with a Tyr residue.) Of the three dioxanes that do not interact with a Tyr, two are found near other side-chain rings, those of His and Phe (Fig. 5*B*). Thus, six of seven enzyme-bound dioxanes are located near rings, with a dioxane oxygen apparently interacting with the ring (Fig. 5). In contrast, the acetonitrile molecules exhibit no such preference for binding at the crystal contacts (only 2 of the 12 acetonitriles bind in such regions), nor do they appear to favor association with ring structures.

In summary, in the present study we have demonstrated that the crystal structures of subtilisin in two unrelated organic solvents, dioxane and acetonitrile, are virtually identical to each other and to that in water. In particular, the active site structures in all three solvents are essentially the same. Also, the overall exposed surface area of the protein in the crystal is not substantially affected by the solvent. With respect to the bound solvent, two dioxane molecules bind in the active site of the enzyme, and the other five are all involved in interprotein crystal contacts. Finally, the dioxane binding sites observed in the enzyme are distinct from those for acetonitrile.

This work was financially supported by National Institutes of Health Grant GM39794.

1. Koskinen, A. M. P. & Klibanov, A. M., eds. (1996) *Enzymatic Reactions in Organic Media* (Blackie, London).
2. Fitzpatrick, P. A., Steinmetz, A. C. U., Ringe, D. & Klibanov, A. M. (1993) *Proc. Natl. Acad. Sci. USA* **90,** 8653–8657.
3. Fitzpatrick, P. A., Ringe, D. & Klibanov, A. M. (1994) *Biochem. Biophys. Res. Commun.* **198,** 675–681.
4. Yennawar, N. H, Yennawar, H. P. & Farber, G. K. (1994) *Biochemistry* **33,** 7326–7336.
5. Yennawar, H. P., Yennawar, N. H. & Farber, G. K. (1995) *J. Am. Chem. Soc.* **117,** 577–585.
6. Allen, K. N., Bellamacina, C. R., Ding, X., Jeffery, C. J., Mattos, C., Petsko, G. A. & Ringe, D. (1996) *J. Phys. Chem.* **100,** 2605–2611.
7. Wescott, C. R., Noritomi, H. & Klibanov, A. M. (1996) *J. Am. Chem. Soc.* **118,** 10365–10370.
8. Ke, T., Wescott, C. R. & Klibanov, A. M. (1996) *J. Am. Chem. Soc.* **118,** 3366–3374.
9. Schmitke, J. L., Wescott, C. R. & Klibanov, A. M. (1996) *J. Am. Chem. Soc.* **118,** 3360–3365.
10. Neidhart, D. J. & Petsko, G. A. (1988) *Protein Eng.* **2,** 271–276.
11. Laitinen, H. A. & Harris, W. E. (1975) *Chemical Analysis* (McGraw–Hill, New York), 2nd Ed., pp. 361–363.
12. Collaborative Computational Project, Number 4 (1994) *Acta Crystallogr. D* **50,** 760–763.
13. Navaza, J. (1994) *Acta Crystallogr. D* **50,** 157–163.
14. Brünger, A. T. (1992) *Nature (London)* **355,** 472–475.
15. Brünger, A. T., Kuriyan, J. & Karplus, M. (1987) *Science* **235,** 458–460.
16. Jones, T. A., Zou, J. Y., Cowan, S. W. & Kjeldgaard, M. (1991) *Acta Crystallogr. A* **47,** 110–119.
17. McRee, D. E. (1993) *Practical Protein Crystallography* (Academic, San Diego), pp. 226–227.
18. Buschmann, J., Müller, E. & Luger, P. (1986) *Acta Crystallogr. C* **42,** 873–876.
19. Bode, W., Papamokos, E. & Musil, D. (1987) *Eur. J. Biochem.* **166,** 673–692.
20. Connolly, M. L. (1983) *Science* **221,** 709–712.
21. Hartsough, D. S. & Merz, K. M., Jr. (1992) *J. Am. Chem. Soc.* **114,** 10113–10116.
22. Hartsough, D. S. & Merz, K. M., Jr. (1993) *J. Am. Chem. Soc.* **115,** 6529–6537.
23. Wescott, C. R. & Klibanov, A. M. (1993) *J. Am. Chem. Soc.* **115,** 1629–1631.
24. Voet, D. & Voet, J. G. (1995) *Biochemistry* (Wiley, Somerset, NJ), 2nd Ed., pp. 398–400.
25. Giegé, R. & Ducruix, A. (1992) in *Crystallization of Nucleic Acids and Proteins*, eds. Ducruix, A. & Giegé, R. (Oxford Univ. Press, New York), pp. 1–18.
26. Mattos, C. & Ringe, D. (1996) *Nat. Biotechnol.* **14,** 595–599.
27. Enge, R. A. & Huber, R. (1991) *Acta Crystallogr. A* **47,** 392–400.